ORIGINAL RESEARCH

ZIF-8 Modified Polypropylene Membrane: A Biomimetic Cell Culture Platform with a View to the Improvement of Guided Bone Regeneration

Fatemeh Ejeian[1,2]
Amir Razmjou[1,3]
Mohammad Hossein Nasr-Esfahani[2]
Munirah Mohammad[3]
Fereshteh Karamali[2]
Majid Ebrahimi Warkiani[4]
Mohsen Asadnia [5]
Vicki Chen[6]

[1]Department of Biotechnology, Faculty of Biological Science and Technology, University of Isfahan, Isfahan 73441-81746, Iran; [2]Department of Animal Biotechnology, Cell Science Research Center, Royan Institute for Biotechnology, ACECR, Isfahan, Iran; [3]UNESCO Center for Membrane Technology, School of Chemical Engineering, University of New South Wales, Sydney, NSW, 2052, Australia; [4]School of Biomedical Engineering, University of Technology Sydney, Sydney, NSW, 2007, Australia; [5]School of Engineering, Macquarie University, Sydney, NSW, 2109, Australia; [6]School of Chemical Engineering, University of Queensland, Brisbane, QLD, 4072, Australia

Correspondence: Amir Razmjou
UNESCO Center for Membrane Technology, School of Chemical Engineering, University of New South Wales, Sydney, NSW 2052, Australia
Tel +61 (2) 9385 4341
Fax +61 (2) 9385 5966
Email amirr@unsw.edu.au

Mohammad Hossein Nasr-Esfahani
Department of Animal Biotechnology, Cell Science Research Center, Royan Institute for Biotechnology, ACECR, Isfahan, Iran
Tel +98 31 95015680
Fax +98 31 95015687
Email mh.nasr-esfahani@royaninstitute.org

Purpose: Despite the significant advances in modeling of biomechanical aspects of cell microenvironment, it remains a major challenge to precisely mimic the physiological condition of the particular cell niche. Here, the metal–organic frameworks (MOFs) have been introduced as a feasible platform for multifactorial control of cell-substrate interaction, given the wide range of physical and mechanical properties of MOF materials and their structural flexibility.

Results: In situ crystallization of zeolitic imidazolate framework-8 (ZIF-8) on the polydopamine (PDA)-modified membrane significantly raised surface energy, wettability, roughness, and stiffness of the substrate. This modulation led to an almost twofold increment in the primary attachment of dental pulp stem cells (DPSCs) compare to conventional plastic culture dishes. The findings indicate that polypropylene (PP) membrane modified by PDA/ZIF-8 coating effectively supports the growth and proliferation of DPSCs at a substantial rate. Further analysis also displayed the exaggerated multilineage differentiation of DPSCs with amplified level of autocrine cell fate determination signals, like *BSP1, BMP2, PPARG, FABP4, ACAN*, and *COL2A*. Notably, osteogenic markers were dramatically overexpressed (more than 100-folds rather than tissue culture plate) in response to biomechanical characteristics of the ZIF-8 layer.

Conclusion: Hence, surface modification of cell culture platforms with MOF nanostructures proposed as a powerful nanomedical approach for selectively guiding stem cells for tissue regeneration. In particular, PP/PDA/ZIF-8 membrane presented ideal characteristics for using as a barrier membrane for guided bone regeneration (GBR) in periodontal tissue engineering.

Keywords: metal–organic framework, mesenchymal stem cell, ZIF-8, cell culture platform, barrier membrane

Introduction

Since the first cell clinical trial on adult mesenchymal stem cells (MSCs) in 1995, these cells have been applied to a wide array of defects, primarily including neurodegenerative diseases,[1] eye disorders,[2] cardiovascular diseases,[3] cartilage and intervertebral disc destruction,[4] bone loss,[5,6] autoimmune disorders,[7] and oral and maxillofacial reconstruction.[8] Dental-related stem cells (like dental pulp stem cells (DPSCs), stem cells from exfoliated deciduous teeth (SHEDs), stem cells from

apical papilla (SCAPs) and periodontal ligament stem cells (PDLSCs)) are considered as promising stem cell sources, thanks to their accessibility, noninvasive harvesting, neural crest origin, and exceptional plasticity.[9] Human DPSCs are reported to have a capability to contribute to the regeneration of a large array of tissues ranging from oral and maxillofacial defects,[10] to corneal disease,[11] and pancreatic islet.[12] Despite remarkable progress toward the biomedical application of stem cells,[13,14] isolation, expansion, and differentiation of MSCs under clinical conditions are still challenging.[15]

Conventional regenerative procedures are typically associated with the use of biological components that causes serious concerns for translating basic scientific reports from the bench to patient care. Predominantly, batch-to-batch variability, xenogenic contaminants, and costly manufacturing on a large scale currently present challenges to the use of existing regenerative protocols (as reviewed by Adam D. et al[16] and Tan and Barker).[17] Moreover, typical tissue engineering strategies rely on the use of proper scaffolds to support critical behavior of the cells and provide essential mechanical parameters of natural tissues.

Accordingly, there has recently been a tendency toward the regulation of physical and biological behaviors of stem cells by controlling the properties of the substrate materials that interact with the cells.[18–20] In contrast to conventional plastic or glass culture substrates, tailored biomaterials present the ability to mimic different physical and mechanical properties of tissue microenvironments.[21–23] They can directly/indirectly activate different transcriptional programs and trigger specific responses in associated cells.[24] In fact, this occurs in a dynamic interaction between cells and the substrate through which cells sense substrate signals and redefine their surrounding environment overtime via secretion of a wide range of matrix components and growth factors.[25–27]

Therefore, a broad range of biomaterials has been exploited, which commonly include natural or synthetic hydrogels,[28] electrospun polymeric fibers,[29] and patterned plastic or glass-based substrates. In particular, paper-based cell culture platforms have become increasingly popular for in vitro expansion of cells as well as biomedical applications, like designing anti-biofouling membranes,[30] biosensors,[31,32] tissue regeneration, drug screening, and disease modeling.[33] The biocompatibility, porous and flexible structure, low-cost, and easy high-throughput manufacturing make paper scaffolds the ideal subjects for

construction of complex tissues. For instance, resorbable/non-resorbable bioactive barrier membranes are extensively utilized in guided bone regeneration (GBR), for preventing invasion of non-osteogenic cells to defect site.[34,35] Some recent clinical and preclinical studies reported reasonable improvement in cell adhesion, proliferation and osteopromotion by use of polypropylene (PP) membrane for alveolar defects.[36–39] The PP membrane is an impermeable porous platform with high rigidity and elastic memory.[40] Owing to its hydrophobic nature, PP membrane could provide isolated spaces for regeneration of damaged tissues through minimizing infiltration of cells and biomolecules. However, the pristine PP membrane is not favorable for adhesion, organization, and proper activity of proteins/cells, underline the importance of surface modification approaches for expanding its biomedical application.[41,42]

Besides the inherent chemical properties of biomaterials, various physical and mechanical parameters, such as stiffness,[43–45] topography,[46–48] viscosity,[49] density,[33,50] cellular internalization,[51] degradation rate,[52] and biomaterial groups[53–55] have been applied to control stem cell behaviors including viability, proliferation, motility, spreading and differentiation capacity (extensively reviewed in Ref).[20,56–58] For example, it is now clear that the gradient of substrate stiffness in physiological condition effectively regulates the essential activity of cells and has a profound influence on their fate.[28,59–61] Moreover, micro- and nano-scale roughness can directly affect the cellular behavior of MSCs, such that various structural features of the materials regulate the proliferation or differentiation potential of the cells.[62–64] In addition, the level of surface hydrophilicity selectively controls the tendency of cells to attach and spread on the substrate, which alters cellular activities by interfering with integrin-related signaling pathways.[65–67]

It is of paramount importance to note that the existing approaches usually target cell microenvironment via altering a single key factor, rather than reconstitution of a whole-cell niche (reviewed by Tewary et al).[68] Although some more recent studies gained higher efficiency and more specificity via a combination of two distinct approaches,[69–72] there is still a big gap to comprehensive mimicry of the natural physical and mechanical condition of cells.

Metal-organic frameworks (MOFs) have been used in wide-ranging applications, such as gas storage and separation,[73–76] molecular sieving,[77,78] sensing,[79–82] and catalysis.[83–85] Because of their impressive capacities,

MOFs have emerged as a promising material type for various biomedical applications, especially in drug delivery and biosensing platforms (reviewed in Ref).[35,86,87] Moreover, recent progress in designing and manufacturing of MOF nanostructures leading to their novel biomedical applications, such as osteogenesis promotion,[88–90] photosensitizer,[91] biomolecule vehicle,[92] Intracellular sensing,[93,94] bioimaging,[95] and biocatalysis.[96] They are highly ordered porous materials composed of metal coordination centers connected by organic linkers.[97] Among them, zeolitic imidazolate frameworks (ZIFs) have attracted intense interest due to their impressive stability along with their high porosity and surface area. They are generally composed of tetrahedrally coordinated metal ions (M= Zn^{2+}, Co^{2+}, Cd^{2+}, Mg^{2+}, etc.) and imidazolate derivatives (Im).

MOFs are porous structures, which typically have exhibited considerable stability in physiological conditions and possess a good potential for in situ- and post-synthetic functionalization with certain biomolecules, either on metals or organic ligands.[98–100] Namely, Immobilization of enzyme-MOF composites on porous and flexible membranes introduces an effective approach for designing bioactive substrates.[101,102] Moreover, MOFs serve as an ideal host for adsorption and conjunction of short peptides, antibodies, and nucleic acids (reviewed by Kempahanumakkagari et al).[103] These merits make the MOF layers well suitable for supporting the cellular behaviors through both in vitro and natural conditions.

Additionally, using various metal groups and numerous organic molecules, MOFs form a wide range of structures with a highly tunable pore size (usually 0.4–6 nm) and surface area (500–4500 m^2/g).[104,105] Different configuration, porosity, and functionality of MOFs can be achieved by controlling framework interpenetration.[106] Also, size of particles could be precisely adjusted by controlling effective parameters in synthesis procedures or applying different mechanisms.[107,108] They are composed of a permanent pore space which can adsorb guest molecules via changing in unit cell volume or subnetwork displacement. For example, ZIF-8 can absorb larger guest molecules by linker rotation[109] or present modified porous nature under reasonable pressure.[51] These intriguing chemical and structural properties of MOFs make these materials an ideal candidate for mimicking the physical and mechanical characteristics of natural tissue.

Although various strategies have been reported for fabrication of MOF thin layers, in situ crystallization and growth on chemically modified supports is of great interest.[110] Polydopamine (PDA) is a mussel-inspired adhesive polymer, which gives numerous unshared electron pairs for secondary reactions.[111] Recently, PDA-based sticky platforms have been used to attach MOF nutrients on a wide range of organic and inorganic supporting materials.[82,112]

Although MOFs are increasingly set to become useful tools in the biomedical area, their potential to form cell culture substrates is not fully explored yet. In consequence, this paper takes a new look at the capability of the ZIF-8 thin layer to support essential activities of dental pulp stem cells (DPSCs) under in vitro condition. Following the characterization of specific mechanical properties of the PP/PDA/ZIF-8 membrane, we evaluated primary cellular attachment, proliferation rate, and multi-lineage differentiation of cells on this platform. Fundamental behaviors of DPSCs were compared to tissue culture plates (TCP), as the gold standard for cell culture substrates. The ZIF-8 nano structure point to new opportunities for surface functionalization of PP membranes as a nanomedicine with significant advantages for using in GBR therapies.

Materials and Methods
Preparation and Characterization of Modified Membranes

A thin film layer of ZIF-8 was fabricated on a PP substrate, as we documented earlier.[82] In brief, the membranes were cleaned carefully with absolute ethanol and immersed in a fresh solution of polydopamine/poly(ethylene imine) (PDA/PEI, 2mg/mL of each) for 4 hours. Following rinsing with deionized water, the samples were incubated in an aqueous solution of 2.74 mg/mL of $Zn(NO3)_2$ and 56.6 mg/mL of 2-methylimidazole for 2 hours (Scheme 1).

The physical and mechanical properties of the ZIF-8 modified substrates then were assessed in comparison to PDA/PEI coated and intact PP membranes, to characterize the substrates. For this, the surface chemistry of the ZIF-8 layer was evaluated using a Fourier transform infrared spectrometer (Alpha II FT-IR, Bruker, Massachusetts, USA) at a resolution of 4 cm^{-1} in the range of 4000–400 cm^{-1}. X-ray diffraction (XRD) was done using Empyrean Thin-Film XRD Xpert Materials Research Diffractometer (MRD) with the 2-theta method (range $5° -40°$, step size 0.025, 100 s/step) was used to study the crystalline structure of ZIF8 thin layer. High
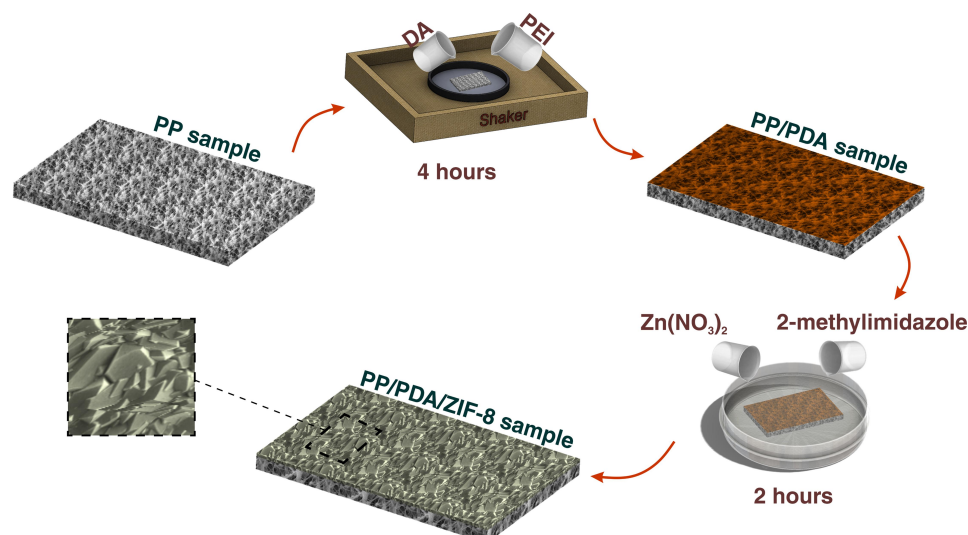
Scheme 1 Schematic presentation of substrate preparation workflow.

Score Plus software was applied for XRD analysis, and peaks were compared with ZIF-8 Database peaks from Powder Diffraction File 4 (PDF-4) organic database (reference ID: 00–062-1030).[113] The morphological and topological characteristics of membranes were also analyzed by scanning electron microscopy (SEM, Zeiss EVO 15LS, Germany). Analysis of surface topography of coated and uncoated specimens was performed in contact mode by using Atomic force microscopy (AFM, JPK NanoWizard 2, Germany).

Furthermore, the static water contact angle was assessed using a Theta optical tensiometer (Biolin Scientific, Sweden) paired with OneAttention software. The surface free energy (SFE) of the membranes was determined by measuring the contact angles of three types of liquids (ie, water, glycerol, di-iodomethane) according to the acid-base Van Oss method. The elastic modulus (stiffness) of the substrates was determined using Bruker Dimension ICON SPM (Bruker Corporation, USA) equipped with an OTESPA-R3 cantilever operated in the PeakForce Tapping mode. The scan size was set to 150 nm with a scan rate of 0.4 Hz, and the resolution of the images was set to 256 samples/line.

Culture and Expansion of DPSCs

Human dental pulp stem cells were obtained and characterized from extracted third molar teeth, as previously described.[114] The experiments were performed under approval of the Ethics Committee of the Royan Institute (NO. IR.ACECR.ROYAN.REC.1397.290), in accordance with the Declaration of Helsinki. Written informed consent

was obtained from all volunteers to participate in the study. Isolated cells were cultured and expanded under standard culture condition, using DMEM medium supplemented with 10% fetal bovine serum (FBS), 1% glutamax, and 1% penicillin/streptomycin (all from Gibco, Paisley, UK). For further experiments, DPSCs (passages 4–6) were seeded with $2.5 \times 10^4/cm^2$ density on substrates, following UV sterilization. Membranes were pre-incubated in complete culture media for overnight, before cell seeding.

Cell Metabolic Activity Assay

To evaluate the viability and proliferation of DPSCs on substrates, the MTS assay was carried out applying cell titer 96 aqueous one solution (Promega, WI, USA) after 8 hours, 1, 3, 5 and 7 days, according to the manufacturer's instruction. Briefly, cultured cells at each time point were incubated with MTS/PMS solution for 3.5 hours. Therefore, the absorbance of produced formazan crystals was measured at 450 nm using a microplate reader (Fluostar Optima, BMG Lab Technologies, Germany) and normalized to the cell-free solution.

Cell Viability Assay

Carboxyfluorescein diacetate succinimidyl ester (CFSE; Sigma, Munich, Germany) was used to evaluate the viability of cultured cells on the ZIF-8 substrate. After one day, the attached cells were incubated with serum-reduced (1% FBS) medium contained five µM CFSE for 30 minutes. Next, the esterase reaction was quenched by adding serum-supplemented (10%) medium, and dead cells were stained

by five μg/mL propidium iodide (PI) for one minute. Imaging by fluorescence microscopy (Olympus, BX51, Japan) showed live DPSCs as green CFSE labeled cells, while dead cells were counterstained with PI.

Morphological and Cytoskeletal Analysis of DPSCs

Cultured substrates were examined by SEM on day 1, to monitor the morphological features of DPSCs. Before imaging, cells were fixed in 2.5% glutaraldehyde and dehydrated with increasing concentration of ethanol.

To visualize the cells' cytoskeleton, F-actin microfilaments were stained at day one and seven post-seeding, by using phalloidin-TRITC; following fixation with 4% paraformaldehyde and permeabilization by 0.2% Triton X-100 (all from Sigma, Munich, Germany). Cell nuclei were counterstained with DAPI (Sigma, Munich, Germany), and monitored under fluorescence microscopy (Olympus, BX51, Japan). The number of cells was quantified by counting the DAPI-stained nuclei from five random low-magnification fields. Cell spread area was also measured in images by applying Image J software (Version 1.42q, National Institutes of Health, USA).

Evaluation of Differentiation Potential

To gain more insights on the ability of DPSCs to differentiate into different lineages on the substrate of ZIF-8, a confluent monolayer of cells was maintained with specific induction media. Briefly, osteogenesis was promoted by facing cells with normal culture medium containing 50 mg/mL ascorbic acid, 10 mM β-glycerophosphate, and 10 nM dexamethasone. Adipogenic induction was also carried out using growth medium supplemented with 100 nM dexamethasone, 50 μg/mL β-glycerophosphate, and 50 μg/mL indomethacin. Further, chondrogenesis was induced via DMEM medium enriched with 10 ng/mL TGFB1, 100 nM dexamethasone, 50 μg/mL ascorbic acid, 100 μg/mL sodium pyruvate, 40 μg/mL L-proline, 1% ITS and 1% FBS.

Following three weeks induction, the level of differentiation was quantified using qRT-PCR for lineage-specific markers (osteogenesis: osteopontin (*OPN/BSP1*) and bone morphogenetic protein 2 (*BMP2*), adipogenesis: peroxisome proliferator-activated receptor gamma (*PPARG*) and fatty acid binding protein 4 (*FABP4*), and chondrogenesis: collagen 2 (*COL2A1*) and aggrecan (*ACAN*)). All specific gene expressions were normalized to *GAPDH* housekeeping gene

(See Supplementary Table 2 for details). Total RNA was extracted using TRIzol reagent (Invitrogen, CA, USA), and cDNA synthesis was carried out by applying the Amplisense cDNA Synthesis kit (AmpliSens, Moscow, Russia). qRT-PCR reactions were done by Applied Biosystems Step One Plus (ABI, CA, USA) and data analysis performed through the ddCt method to compare to pre-treatment cells (day 0).

In addition, an immunocytochemistry assay was carried out for further evaluation of differentiation at the protein level. Cells were stained with integrin-binding sialoprotein (IBSP/BSP2), PPARG, and COL2A1, which are used for labeling osteoblasts, adipocytes, and chondrocytes, respectively. To prepare samples for immunostaining, cells were fixed, permeabilized (as we mentioned in section 5.5), and stained with specific primary and secondary antibodies (see Supplementary Table 3 for details). Imaging was performed using fluorescence microscopy (Olympus, BX51, Japan).

Results
Substrate Characterization

A thin layer of ZIF-8 crystals was observed in coated samples, through SEM imaging of modified membranes, and verified by XRD analysis and FTIR absorbance spectra (Figure 1A–C). Even though PP and PP/PDA specimens do not present crystalline XRD pattern, exhibited diffraction peaks of PP/PDA/ZIF8 sample are highly matched with the ZIF8 pattern obtained from Cambridge Structural Database (CSD) as well as the simulated PP/PDA/ZIF8 XRD pattern. PDA/PEI surface modification is accompanied by two distinct IR peaks at 3200–3600 cm^{-1}, due to the stretching vibration of alcohol, catechol and amine bonds, and 1680 cm^{-1}, mainly related to C=N bonds between PEI and PDA. Among new peaks revealed as the result of ZIF8 coating, a characteristic peak at 420 cm^{-1} refers to Zn-N stretching, and the other notable peak at 1600 cm^{-1} corresponds to N-H bending. In addition, substrate treatment with PDA and PDA/ZIF8 coating dramatically decrease the water contact angle from $130^{\circ} \pm 1$ for PP to $54^{\circ} \pm 8$ and $27.8^{\circ} \pm 7$, respectively. In contrast, SFE values rise significantly after PDA treatment and increase further after ZIF8 coating (Figure 1D). Furthermore, we found that PDA/PEI modification leads to a notably smoother substrate (Ra = 57 nm ± 1.6, Rq = 71.4 nm ± 5.8) compared to pristine PP membrane (Ra = 213.9 nm ± 18.5, Rq = 279.7 nm ± 27.3). On the other hand, as expected, ZIF8 in situ crystallization significantly
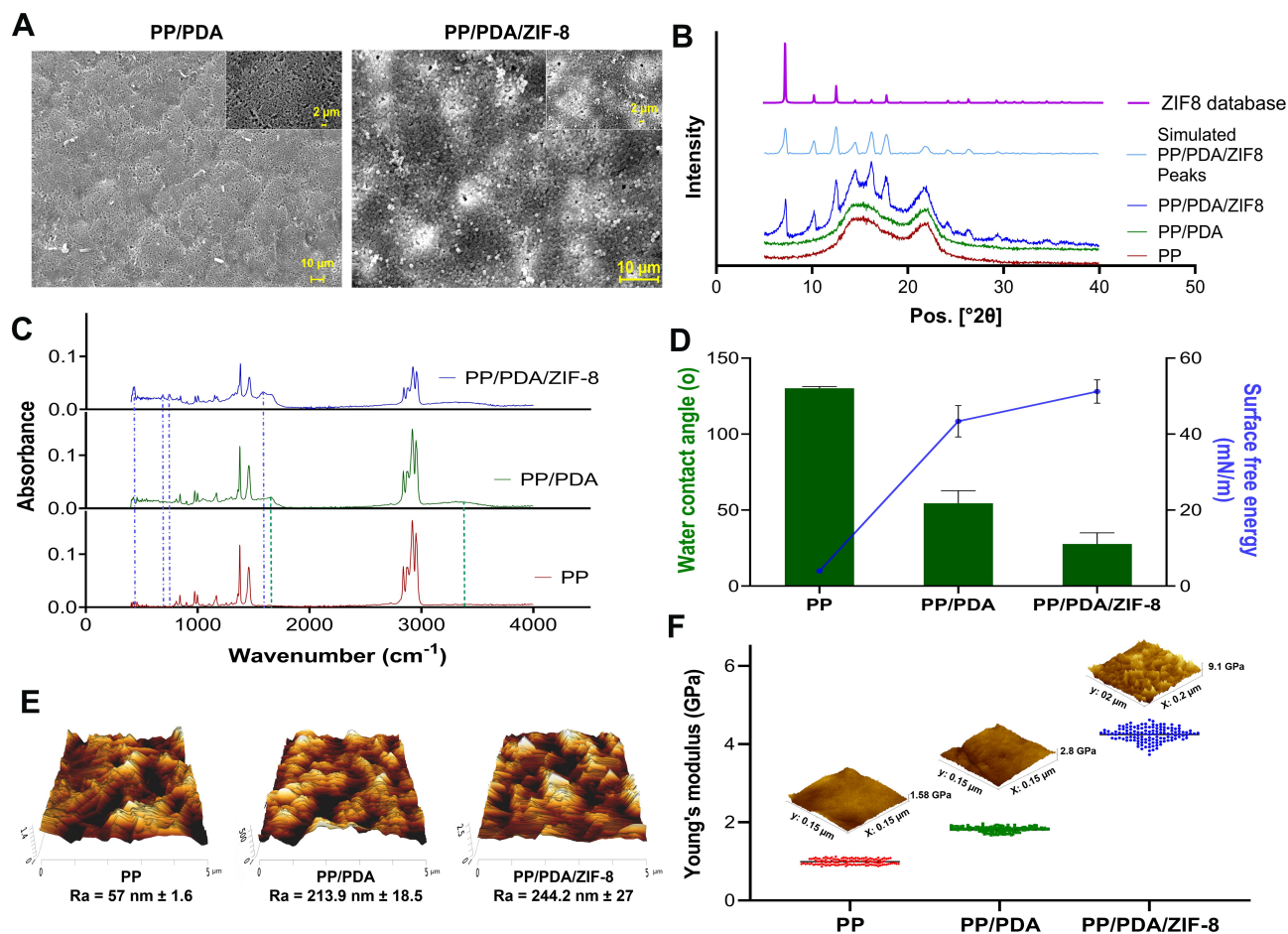
Figure 1 Characterization of modified substrates. (**A**) SEM imaging for exploring the morphological feature of PP/PDA and PP/PDA/ZIF-8 substrates. Images with higher magnification are shown as inserts. (**B**) XRD crystalline patterns of the PP, PP/PDA, and PP/PDA/ZIF-8 membranes compared to the simulated ZIF-8 coated sample and ZIF-8 database. (**C**) FTIR spectra obtained from PP, PP/PDA, and PP/PDA/ZIF-8 samples. Blue and green dash lines show characteristic peaks for ZIF-8 and PDA-PEI, respectively. (**D**) Water contact angle measurement and calculated surface free energy for PP, PP/PDA, and PP/PDA/ZIF-8. Each sample was assessed in three replicates for 10 seconds. Data is represented as mean ± SEM, * p<0.05. (**E**) 3D AFM topographical images and measured surface roughness values of PP, PP/PDA, and PP/PDA/ZIF-8 substrates. (**F**) Surface elastic modulus measurement for PP, PP/PDA, and PP/PDA/ZIF-8 substrates by PeakForce AFM. Individual values are presented for 256 samples/line in each specimen with the corresponding mean value.
Abbreviations: PP, polypropylene; PDA, polydopamine; PEI, polyethyleneimine.

increases the roughness value of the modified membrane (Ra = 244.2 nm ± 27, Rq = 376.3 nm ± 97.1), because of the crystalline structure of the thin layer (Figure 1E). Figure 1F shows 4.25 GPa Young's modulus (from a surface roughness analysis via AFM force mapping) for PP/PDA/ZIF8 samples, which is significantly higher than both PP/PDA (1.84 GPa) and PP (0.99 GPa) specimens.

Cell Attachment on ZIF-8 Thin Film

The first set of cell culture experiments on MOF thin films revealed a proper attachment of DPSCs on PP/PDA/ZIF-8 substrate with a level comparable to the TCP control group (Figure 2A and B). Quantitative analysis showed that nearly twice the amount of cells adhered to ZIF-8, while the spread area of the cells did not change much (Figure 2C). We also

assessed the primary metabolic activity of cells attached to samples by MTS assay. Surprisingly, cells cultured on ZIF-8 exhibited markedly reduced activity, in contrast to the control group of TCP (Figure 2D). Morphological studies by SEM imaging provided additional evidence for satisfactory adherence of cells on ZIF-8, likewise TCP surface (Figure 2E and F). Furthermore, strong evidence of the viability of the attached cells is presented in Figure 2G and H, which shows the high number of CFSE$^+$/PI$^-$ cells on TCP and ZIF-8 layer.

On the other hand, notable populations of cells were found on the intact polypropylene support, which formed an aggregation feature with a very low level of cell spreading. This phenomenon was confirmed by SEM imaging, and the basal activity of cells in this configuration was defined regarding MTS results (Supplementary Figure 2).
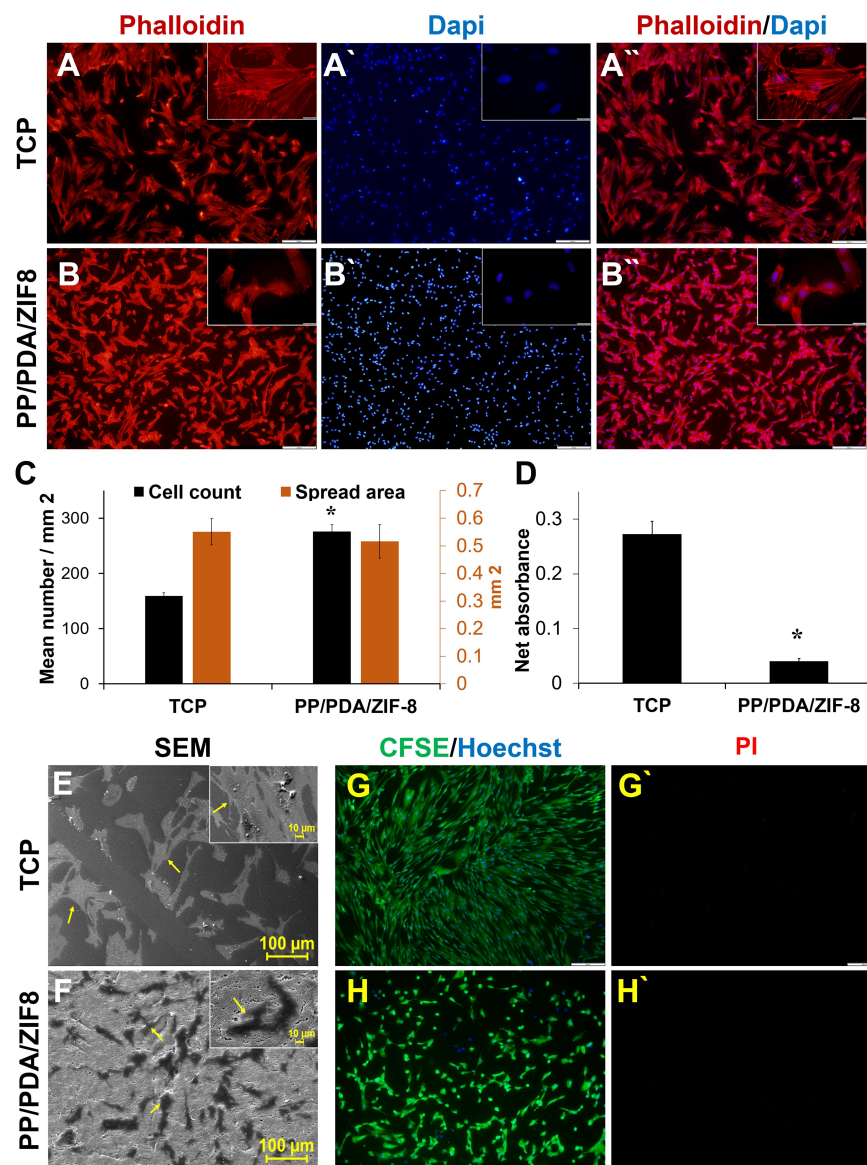
Figure 2 Cellular attachment and viability analysis of DPSCs on the ZIF-8 modified substrate. F-actin arrangement of DPSCs cultured on (**A**) TCP and (**B**) PP/PDA/ZIF-8 substrates after one day. F-actin filaments were visualized via labeling with phalloidin-TRITC (red), and nuclei were stained with DAPI (blue). Scale bar = 200 μm. Magnified inserts showed the typical morphological features of cells on each substrate. Scale bar = 20 μm. (**C**) Bar graph presenting the quantification of cell count (black bar) and cell spread area (brown bar). (**D**) Analysis of cell metabolic activity was carried out after 8 hours, using MTS assay. SEM imaging of cultured cells on (**E**) TCP and (**F**) PP/PDA/ZIF-8 substrates, following one-day incubation in normal culture condition. The viability of cultured DPSCs was evaluated on (**G**) TCP and (**H**) PP/PDA/ZIF-8 substrates on day 1. Viable cells are stained in green as the result of CFSE cleavage, while dead cells are showed by PI-positive cells (red points). Quantified data are represented as mean ± SEM from three independent experiments, * $p < 0.05$.

Not surprisingly, DPSCs finely attached, extended, and retained their fibroblastic morphology on PDA modified PP membrane (Supplementary Figure 3).

Cell Proliferation on Modified Membranes

As for TCP, cytoskeletal imaging of cells on PP/PDA/ZIF-8 substrate after seven days clearly showed the significant propagation of cells in comparison to the first day (Figure 3A and B). Further quantitative analysis of

figures highlighted that a greater number of cells with a higher spread area were observed on the ZIF-8 layer than for a standard tissue culture plate (Figure 3C). Aligned with these findings, MTS analysis revealed a reasonable absorbance on day one through both tested groups, which gradually rose to a near-constant (Figure 3D). While the TCP group showed higher initial absorbance and peaked sooner (day 5), cells on PP/PDA/ZIF-8 coated membrane grew rapidly, as overtaking the control after seven days.
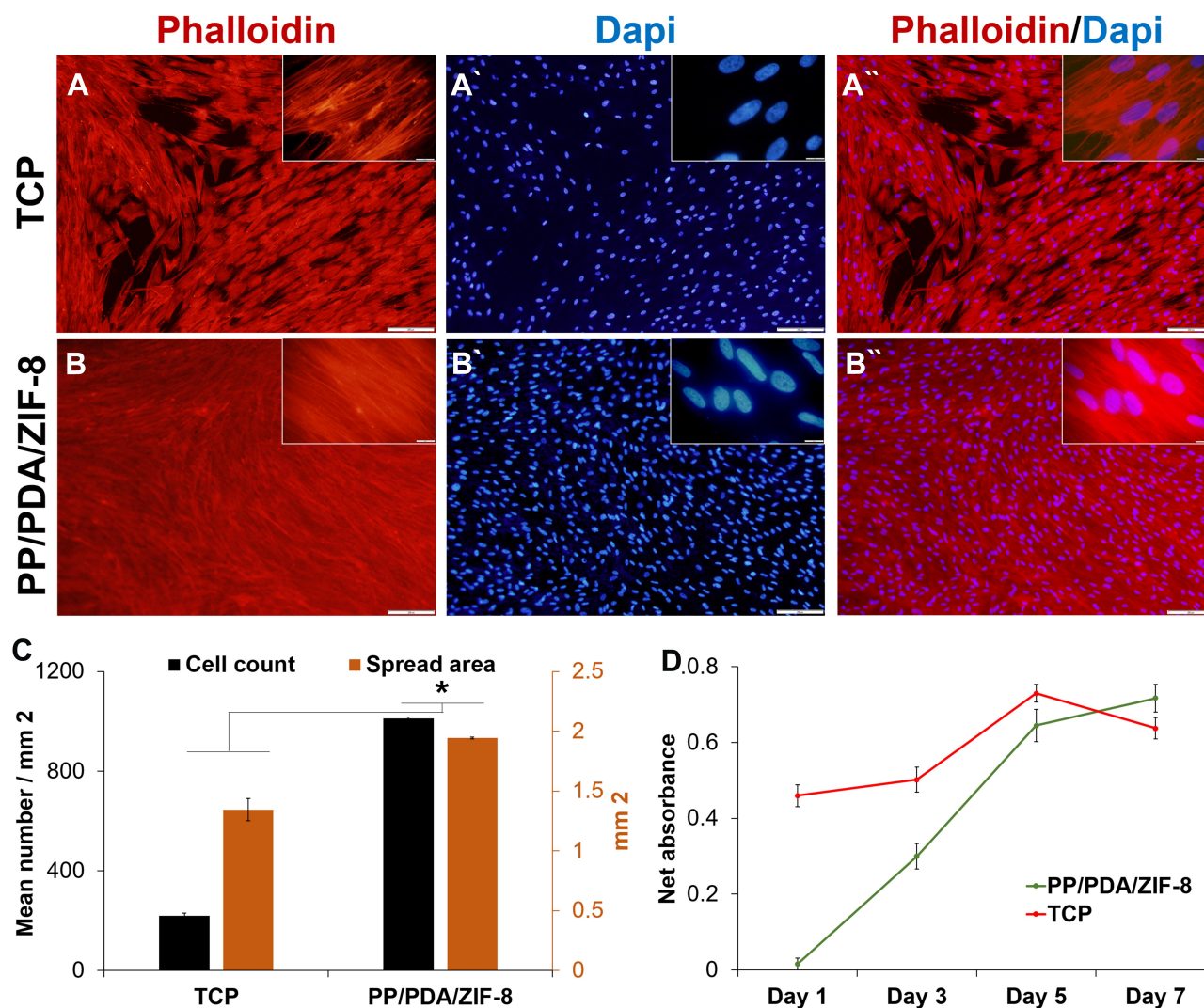
Figure 3 Proliferation potential of DPSCs on the ZIF-8 modified substrate. Cytoskeletal F-actin staining of DPSCs cultured on (**A**) TCP and (**B**) PP/PDA/ZIF-8 substrates after seven days. F-actin filaments were visualized via labeling with phalloidin-TRITC (red), and nuclei were stained with DAPI (blue). Scale bar = 200 μm. The insets are showing a higher-magnification view of the larger image. Scale bar = 20 μm. (**C**) Quantification analysis of cell number (black bar) and cell spread area (brown bar) of phalloidin-stained cells after a week. (**D**) Investigation of the proliferation rate of cultured DPSCs via analysis of cellular metabolic activity with MTS assay over seven days.

Even though cellular activity and the total spreading of DPSCs attached to the PP membrane displayed slight elevation during the period, the overall number of cells did not increase (Supplementary Figure 2). On the other hand, Supplementary Figure 3 provides evidence on the proliferation and expansion of DPSCs on the PP/PDA modified membrane.

Multilineage Differentiation of DPSCs on ZIF-8-Coated Membranes

The multilineage differentiation potential of DPSCs on the ZIF-8 layer was assessed following 3-weeks induction under specific culture conditions. Gene expression analysis exhibited significant elevation of expression of all critical lineage-specific markers in cells cultured on PP/PDA/ZIF8 in both RNA and protein levels. We found a substantially higher expression level of *BSP1* and *BMP2* not only concerning day 0 (external control sample) but also to the treated cells on the TCP substrate (Figure 4A). On the other hand, the expression of *PPARG* and *FABP4* enhanced with an almost similar level in both experimental groups (Figure 4B). Interestingly, two-dimensional chondrogenic induction resulted to form an aggregation of cells exceptionally expressed *COL2A1* and *ACAN*; however, it was much fewer than the cells cultured on TCP (Figure 4C). Immunofluorescent imaging also revealed considerable expression of BSP2, PPARG, and COL2A1 in DPSCs, which were treated with osteo-, adipo-, and
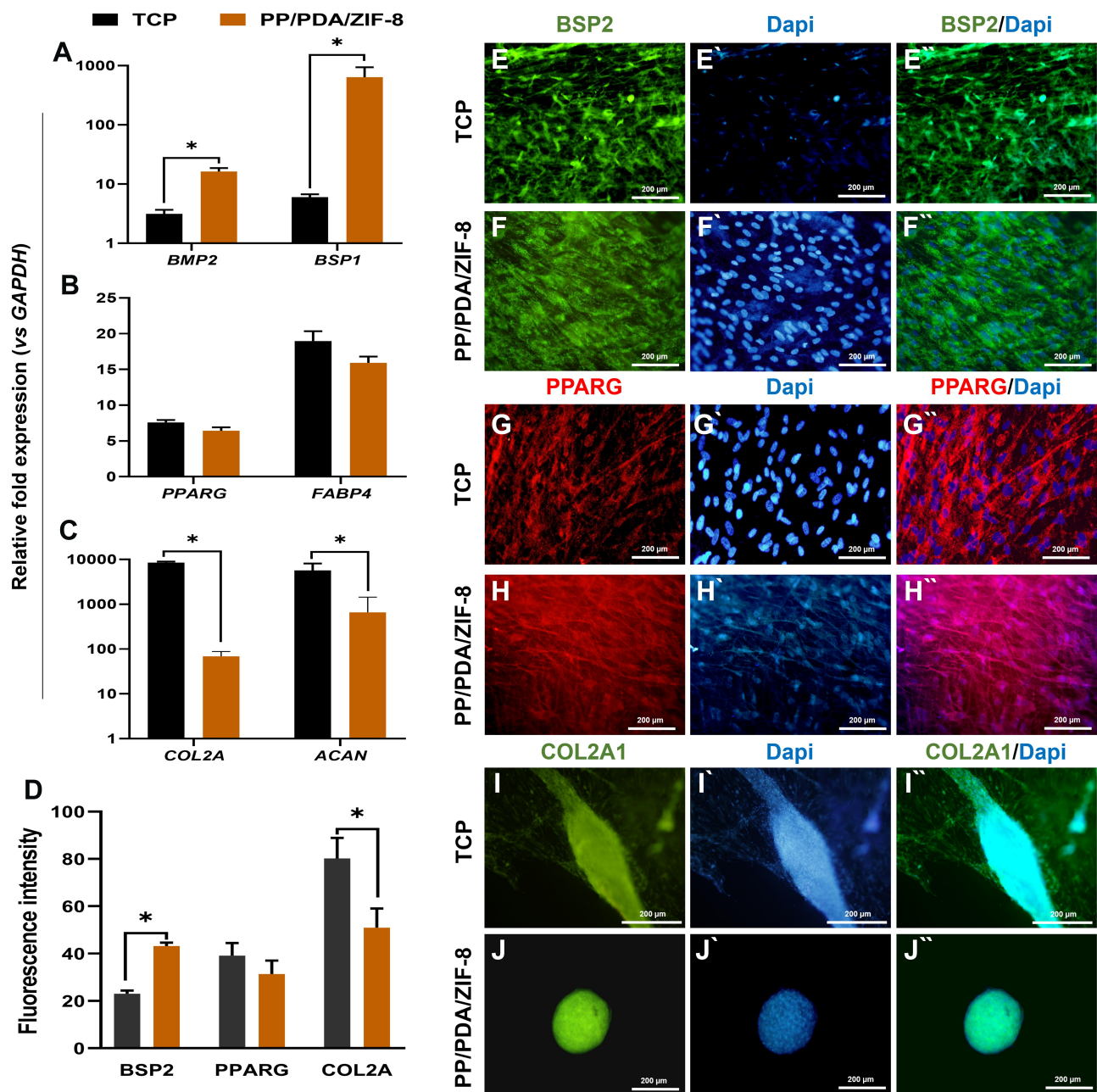
Figure 4 Multilineage differentiation potential of DPSCs on the ZIF-8 modified substrate. Evaluation of the multilineage differentiation potential of DPSCs cultured on PP/PDA and PP/PDA/ZIF-8, and TCP substrates at mRNA level, after three weeks induction. Osteo-, adipo-, and chondrogenesis were assessed respectively via measurement of the relative expression of (**A**) *BSP1* and *BMP2*, (**B**) *FABP4* and *PPARG*, and (**C**) *COL2A1* and *ACAN* compared to pre-treated cells (Day 0). Data represented as mean ± SEM from three independent experiments, * p<0.05. (**D**) The quantitative analysis of fluorescence intensity of immunostaining assay for lineage-specific markers (BSP2: Osteoblasts; PPARG: Adipocytes; COL2A1: Chondrocytes) in the level of protein at the end of 21 days induction time for DPSCs cultured on TCP and PP/PDA/ZIF-8. The representative images of stained DPSC for (**E, F**) BSP2, (**G, H**) PPARG, and (**I, J**) COL2A1. In all images, nuclei were stained in blue with DAPI. Scale bar is 200 μm.

chondrogenic induction medium on TCP and PP/PDA/ZIF-8 substrate (Figure 4D–J).

Discussion

Despite rapid progress toward the biomedical application of stem cells, there remains a high demand for clinical-grade stem cell products as well as functional supports to promote tissue regeneration. Over the past two decades, bioengineering strategies investigate for suitable biomaterials to develop safe patient-specific regeneration therapies. In line with our previous studies,[77,82,101,102,110,115] we proposed these nanostructures as tunable cell culture platforms with considerable potential to simultaneously regulating different microenvironmental cues.

This idea is supported by the diverse physical and mechanical characteristics of more than 20,000 components belong to MOF family, such as elastic properties, inherent porosity, stiffness, and particle size.[116,117] From the literature, it is mainly governed by the structural flexibility, framework breathing, and the chemistry of subunits, and influenced by the fabrication conditions.[117–119] Besides, there are very limited reports exploited particular characteristics of MOFs to specifically control cellular behavior. For instance, controllable gas-release from photoactive MOF crystals has been applied for local regulation of cellular signaling pathways through in vitro culture conditions.[120,121] A number of recent approaches have utilized MOF nanoparticles for improving osteoconductivity/osteoinductivity of standard bone substituents, such as titanium (Ti), poly-l-lactic acid (PLLA), and calcium phosphate (CaP).[88,89,122] This emerging paradigm is quite governed by the precise concentration of metal ions and the stability of MOF nanostructure. Accordingly, it is deduced that applying MOF layers could improve their stability at the cell-substrate interaction surface and decline their probable toxic effect.

According to our hypothesis, we examined the cellular response of human DPSCs to the particular physio-mechanical cues of the ZIF-8 thin layer, as a well-known example of MOFs. All experiments were also performed for the PP membrane as well as PP/PDA to ascertain whether the findings were related to the ZIF-8 layer. Razmjou et al previously investigated the physical properties of the ZIF-8 dense layer with an approximate thickness of 800 nm and sensible adsorption capacity for silver particles.[82] Generally, this study showed that forming the ZIF-8 layer significantly improved the hydrophilicity, SFE, nano-roughness, and elastic modulus of the PP membrane. Indeed, the chemical composition analysis identified plenty of N-H and Zn-N bonds in the ZIF-8 crystalline layer.

Based on the critical objectives of tissue engineering, cell culture platforms are required to hold suitable surface properties to promote stem cell adhesion, proliferation, and differentiation.[123–125] The higher number of adhered DPSCs on the ZIF-8 layer, as compared to TCP as the "gold standard" substrate for cell culture, highlights its superiority not only for in vitro but also for in vivo and clinical experiments. In fact, the relative increased roughness and greater surface area provided by ZIF-8 film (37.46 m^2/g, graphs are shown in Supplementary Figure 1 and data are summarized in Supplementary Table 1) along with the active basic nitrogen atoms in the structure of ZIF-

8 crystals seems to play critical roles in the primary attachment of cells.[126]

Although DPSCs were successfully attached to a ZIF-8 layer, they were not able to expand very well and find an appropriate fibroblastic morphology within one day. The reduced level of metabolic activity at this stage correlates with substantial evidence in the literature that showed the reduced cell spreading area, indicating a significant drop in cellular metabolism.[127–129] Interestingly, after seven days, they formed a compact monolayer of cells that overtook the PP/PDA group and TCP. Furthermore, the significant higher surface free energy is also an essential factor for enhanced cell attachment following PDA modification. This result is in accordance with reported findings that considered surface free energy as an effective parameter for cell-substrate interaction, in addition to wettability.[130]

Regarding the importance of efficient differentiation promotion by cell culture platforms through homing conditions,[131–133] we evaluated the multilineage potential of DPSCs during long-term culturing on a ZIF-8 layer. It is suspected that considerable upregulation in all three lineage-related genes is at least partially related to the higher surface area provided by the ZIF-8 layer. Even more important factor may be harnessing of cell-secreted stimulatory signals by internal active sites in the ZIF-8 crystalline layer.[99] The trapping of soluble growth factors and ECM components secreted by differentiating DPSCs on the substrate resulting in subsequent amplification of the differentiation process.

As a key index of osteogenic differentiation during bone development and regeneration,[134,135] the highly amplified expression of *BSP1* and *BMP2* on PP/PDA/ZIF-8 platform is in line with our primary hypothesis on promising potential of the ZIF-8 layer for exaggerating the innate osteogenic potential of DPSCs. Indeed, our findings showed that the ZIF-8 coating drastically increased the rigidity of matrix, which is extensively reported to have a major impact on the commitment of MSCs to osteogenic differentiation.[37,136,137] The higher elastic modulus of PP/PDA/ZIF-8 substance compared to the reported value for standard tissue culture plates (≈ 1 GPa) is consistent with the higher level of osteogenesis on the ZIF-8 layer.[138,139] Stiff materials predominantly regulate cell fate via modulating integrin interactions, reorganizing adhesion ligands, increasing cytoskeletal tension,[140] and inducing epigenetic modification.[141]

As a result of the chondrogenic induction of DPSCs through two-dimensional culture conditions, we were

surprised to detect 3D cartilage-like structures after three weeks. This finding is in complete agreement with the proper physiological environment of chondrocytes, which function in loose contact with the substrate.[142–144] It seems that the stiff surfaces provided by both test and control groups prompted the cells to disrupt cell-substrate adhesions, migrate, and form features more resembling the natural cartilage environment. The elevated expression of COLL2A confirmed the notable level of chondrogenesis on both substrates. The higher stiffness value of PP/PDA/ZIF-8 is accompanied by lower chondrogenic efficiency, compared with TCP. In contrast to remarkable osteo- and chondrogenesis, the relative weaker adipogenic differentiation observed maybe because of the stiff structure of the substrates.

Hence, these attractive features render PP/PDA/ZIF-8 platform suitable for GBR therapies. GBR is a surgical technique that occludes the in-growth of adjacent soft tissue into periodontal bone defects via utilizing a flexible bioactive barrier membrane. The ideal GBR membrane is required to improve bone regeneration and appropriately integrate into the host tissue.[34] The recent clinical studies provided evidences for recruitment of cells into pristine PP membrane during GBR processes.[38,39,145] Similarly, we found that DPSCs can be attached on PP membrane and enhanced their metabolic activity over time; however, they did not spread properly even after seven days. This phenomenon was also observed for adipose-derived stem cells (ADSCs) grown on poly(l-lactide) acid (PLLA) film.[65] It seems that the inherent hydrophobic characteristic of the support materials strongly inhibited the normal expansion of MSCs in both cases. Whereas, significant improvement in cellular attachment on the PP/PDA/ZIF-8 platform may be reflected in the marked increase in surface hydrophilicity, obtained through PDA surface modification, as previously described by Schendzielorz et al.[146]

Conclusion

In summary, we have obtained satisfactory results proving the promising capacity of ZIF-8 thin film as a stimulating agent on the cell culture substrate. This report opens up a new field of study of the applications of MOFs for the manufacturing of substrates able to mimic various mechanochemical properties of natural tissues. As an example, the PP/PDA/ZIF-8 showed remarkable capacity for the primary adhesion of DPSCs in comparison to other surface modification strategies

(Supplementary Table 4). Exceptional expression of lineage-specific markers on PP/PDA/ZIF-8 substrate, especially in the case of bone-specific markers, presents higher efficiency rather than immobilization of some biological components (Supplementary Table 5). Favorable characteristics of the MOF nanostructures could minimize the requirement for biologically active induction molecules, and provide a chemical-based alternative to cell microenvironments. Further studies should concentrate on designing particular substrates with the desired stiffness, roughness, and geometrical features. On a broader level, we can apply a wide range of post functionalization and pore engineering approaches to mimic physiological conditions. In the light of these findings, PP/PDA/ZIF-8 platform exhibits profound capacity to use as a promising nanomedical tool in GBR procedures, apart from its in vitro application for mimicking natural microstructure of hard tissues.

Disclosure

Ms Fatemeh Ejeian reports grants from the Iran National Science Foundation (INSF) and Biotechnology Development Council of the Islamic Republic of Iran during the conduct of the study. Professor Vicki Chen reports grants from Australian Research Council during the conduct of the study. The authors report no other potential conflicts of interest for this work.

References

1. Volkman R, Concise review: OD. Mesenchymal stem cells in neurodegenerative diseases. *STEM CELLS*. 2017;35(8):1867–1880.
2. Mead B, Logan A, Berry M, Leadbeater W, Scheven BA. Concise review: dental pulp stem cells: a novel cell therapy for retinal and central nervous system repair. *Stem Cells*. 2016;35(1):61–67.

3. Jeong H, Yim HW, Park H-J, et al. Mesenchymal stem cell therapy for ischemic heart disease: systematic review and meta-analysis. *Int j Stem Cells*. 2018;11(1):1–12.

4. Richardson SM, Kalamegam G, Pushparaj PN, et al. Mesenchymal stem cells in regenerative medicine: focus on articular cartilage and intervertebral disc regeneration. *Methods*. 2016;99:69–80.

5. Zhao L, Kaye AD, Kaye AJ, Stem Cell A-EA. Therapy for osteo-necrosis of the femoral head: current trends and comprehensive review. *Curr Pain Headache Rep*. 2018;22(6):41.

6. Grayson WL, Bunnell BA, Martin E, Frazier T, Hung BP, Gimble JM. Stromal cells and stem cells in clinical bone regeneration. *Nat Rev Endocrinol*. 2015;11:140.

7. Gao F, Chiu SM, Motan DAL, et al. Mesenchymal stem cells and immunomodulation: current status and future prospects. *Cell Death Dis*. 2016;7:e2062.

8. Tatullo M, Marrelli M, Paduano F. The regenerative medicine in oral and maxillofacial surgery: the most important innovations in the clinical application of mesenchymal stem cells. *Int J Med Sci*. 2015;12(1):72–77.

9. Botelho J, Cavacas MA, Machado V, Mendes JJ. Dental stem cells: recent progresses in tissue engineering and regenerative medicine. *Ann Med*. 2017;49(8):644–651.

10. Marei MK, El Backly RM. Dental mesenchymal stem cell-based translational regenerative dentistry: from artificial to biological replacement. *Fron Bioeng Biotech*. 2018;6:49. doi:10.3389/fbioe.2018.00049

11. Shangar S, Smith J, Allingham W, et al. Regeneration of corneal epithelium with dental pulp stem cells – an ex-vivo limbal stem cell deficiency model. *Invest Ophthalmol Vis Sci*. 2020;61(7):1203.

12. El-Kersh AOFO, El-Akabawy G, Al-Serwi RH. Transplantation of human dental pulp stem cells in streptozotocin-induced diabetic rats. *Anat Sci Int*. 2020;95(4):523–539. doi:10.1007/s12565-020-00550-2

13. Boregowda SV, Booker CN, Phinney DG. Mesenchymal stem cells: the moniker fits the science. *STEM CELLS*. 2018;36(1):7–10. doi:10.1002/stem.2713

14. Bakopoulou A, Huang GTJ, Rouabhia M, Geurtsen W, Advances AI. New technologies towards clinical application of oral stem cells and their secretome. *Stem Cells Int*. 2017;2017 (2017):6367375.

15. Galipeau J, Mesenchymal Stromal SL. Cells: clinical challenges and therapeutic opportunities. *Cell Stem Cell*. 2018;22(6):824–833.

16. Celiz AD, Smith JGW, Langer R, et al. Materials for stem cell factories of the future. *Nat Mater*. 2014;13:570.

17. Tan S, Barker N. Engineering the niche for stem cells. *Growth factors*. 2013;31(6):175–184.

18. Arnold AM, Holt BD, Daneshmandi L, Laurencin CT, Sydlik SA. Phosphate graphene as an intrinsically osteoinductive scaffold for stem cell-driven bone regeneration. *Proceedings of the National Academy of Sciences*. 2019;116(11):4855.

19. Cipitria A, Salmeron-Sanchez M. Mechanotransduction and Growth Factor Signalling to Engineer Cellular Microenvironments. *Advanced Healthcare Materials*. 2017/08/01 2017;6(15):1700052.

20. Madl CM, Heilshorn SC, Blau HM. Bioengineering strategies to accelerate stem cell therapeutics. *Nature*. 2018;557(7705):335–342.

21. Yan S-R, Zarringhalam M, Toghraie D, Foong LK, Talebizadehsardari P. Numerical investigation of non-Newtonian blood flow within an artery with cone shape of stenosis in various stenosis angles. *Comput Methods Programs Biomed*. 2020;192:105434.

22. Alipour P, Toghraie D, Karimipour A, Hajian M. Molecular dynamics simulation of fluid flow passing through a nanochannel: effects of geometric shape of roughnesses. *J Mol Liq*. 2019;275:192–203.

23. Maleki R, Afrouzi HH, Hosseini M, Toghraie D, Rostami S. Molecular dynamics simulation of Doxorubicin loading with N-isopropyl acrylamide carbon nanotube in a drug delivery system. *Comput Methods Programs Biomed*. 2020;184:105303.

24. Darnell M, O'Neil A, Mao A, Gu L, Rubin LL, Mooney DJ. Material microenvironmental properties couple to induce distinct transcriptional programs in mammalian stem cells. *Proceedings of the National Academy of Sciences*. 2018;115(36):E8368.

25. Freitas-Rodríguez S, Folgueras AR, López-Otín C. The role of matrix metalloproteinases in aging: Tissue remodeling and beyond. *Biochimica et Biophysica Acta (BBA) - Molecular Cell Research*. 2017;1864(11, Part A):2015–2025.

26. Mor-Yossef Moldovan L, Lustig M, Naftaly A, et al. Cell shape alteration during adipogenesis is associated with coordinated matrix cues. *Journal of cellular physiology*. 2019;234(4):3850–3863.

27. Watt FM, Hogan, Brigid LM. Out of Eden: Stem Cells and Their Niches. *Science*. 2000;287(5457):1427.

28. Caliari SR, Burdick JA. A practical guide to hydrogels for cell culture. *Nat Methods*. 2016;13:405.

29. Sharma AD, Zbarska S, Petersen EM, Marti ME, Mallapragada SK, Sakaguchi DS. Oriented growth and transdifferentiation of mesenchymal stem cells towards a Schwann cell fate on micropatterned substrates. *J Biosci Bioeng*. 2016;121(3):325–335.

30. Orooji Y, Liang F, Razmjou A, et al. Excellent biofouling alleviation of thermoexfoliated vermiculite blended poly(ether sulfone) ultrafiltration membrane. *ACS Appl Mater Interfaces*. 2017;9 (35):30024–30034.

31. Changani Z, Razmjou A, Taheri-Kafrani A, Domino P-μmb: AM, New A. Approach for the sequential immobilization of enzymes using polydopamine/polyethyleneimine chemistry and microfabrication. *Adv Mater Int*. 2020;7(13):1901864.

32. Karimi-Maleh H, Karimi F, Orooji Y, et al. A new nickel-based co-crystal complex electrocatalyst amplified by NiO dope Pt nanostructure hybrid; a highly sensitive approach for determination of cysteamine in the presence of serotonin. *Sci Rep*. 2020;10(1):11699.

33. Ng K, Gao B, Yong KW, et al. Paper-based cell culture platform and its emerging biomedical applications. *Materials Today*. 2017;20 (1):32–44.

34. Elgali I, Omar O, Dahlin C, Thomsen P. Guided bone regeneration: materials and biological mechanisms revisited. *Eur J Oral Sci*. 2017;125(5):315–337.

35. Berton F, Porrelli D, Di Lenarda R, Turco G, Critical A. Review on the production of electrospun nanofibres for guided bone regeneration in oral surgery. *Nanomaterials*. 2020;10(1):16.

36. De Oliveira EL, De Carvalho PSP, Da Silva TB. Histological and histomorphometric evaluation of efficacy of a polypropylene barrier in guided bone regeneration and modified guided bone regeneration in critical defects in rodent cranial vaults. *J Indian Soc Periodontol*. 2019;23(4):351–355.

37. De Lucca L, da Costa Marques M, Weinfeld I. Guided bone regeneration with polypropylene barrier in rabbit's calvaria: a preliminary experimental study. *Heliyon*. 2018;4(6):e00651.

38. Esch TH, da Silva Barbirato D, Fogacci MF, de Oliveira Magro O, de Barros MCM. Tissue healing with polypropylene membrane used as conventional guided bone regeneration and exposed to the oral cavity for post-dental extraction: a case report. *Revista Científica Do CRO-RJ*. 2018;3(2):52–56.

39. Pedron IG, Bispo LB, Salomão M. Selective polypropylene membrane: alveolar behavior in post-extraction repair with a view to the future installation of osseointegrated implants. *Practice*. 2018;8:9.

40. Himma NF, Anisah S, Prasetya N, Wenten IG. Advances in preparation, modification, and application of polypropylene membrane. *J Polymer Eng*. 2016;36(4):329–362.

41. Fang S, Zhang Z, Yang H, et al. Mussel-inspired hydrophilic modification of polypropylene membrane for oil-in-water emulsion separation. *Surf Coat Technol*. 2020;403:126375.

42. Etemadi H, Fonouni M, Yegani R. Investigation of antifouling properties of polypropylene/TiO2 nanocomposite membrane under different aeration rate in membrane bioreactor system. *Biotechn Rep*. 2020;25:e00414.

43. Engler AJ, Sen S, Sweeney HL, Discher DE. Matrix elasticity directs stem cell lineage specification. *Cell.* 2006;126(4):677–689.

44. Lee H-p, Stowers R, Chaudhuri O. Volume expansion and TRPV4 activation regulate stem cell fate in three-dimensional microenvironments. *Nature Communications.* 2019;10(1):529.

45. Trappmann B, Gautrot JE, Connelly JT, et al. Extracellular-matrix tethering regulates stem-cell fate. *Nat Mater.* 2012;11(7):642.

46. Dalby MJ, Gadegaard N, Tare R, et al. The control of human mesenchymal cell differentiation using nanoscale symmetry and disorder. *Nat Mater.* 2007;6(12):997–1003.

47. Kang KB, Lawrence BD, Gao XR, Guaiquil VH, Liu A, Rosenblatt MI. The Effect of Micro- and Nanoscale Surface Topographies on Silk on Human Corneal Limbal Epithelial Cell Differentiation. *Scientific Reports.* 2019;9(1):1507.

48. Padiolleau L, Chanseau C, Durrieu S, Ayela C, Laroche G, Durrieu M-C. Directing hMSCs fate through geometrical cues and mimetics peptides. *J Biomed Mater Res A.* 2020;108 (2):201–211.

49. Bennett M, Cantini M, Reboud J, Cooper JM, Roca-Cusachs P, Salmeron-Sanchez M. Molecular clutch drives cell response to surface viscosity. *Proceedings of the National Academy of Sciences.* 2018;115(6):1192.

50. Connelly JT, Garcia AJ, Levenston ME. Interactions between integrin ligand density and cytoskeletal integrity regulate BMSC chondrogenesis. *J Cell Physiol.* 2008;217(1):145–154.

51. Chapman KW, Halder GJ, Chupas PJ, Amorphization P-I. Porosity modification in a metal−organic framework. *J Am Chem Soc.* 2009;131(48):17546–17547.

52. Khetan S, Guvendiren M, Legant WR, Cohen DM, Chen CS, Burdick JA. Degradation-mediated cellular traction directs stem cell fate in covalently crosslinked three-dimensional hydrogels. *Nat Mater.* 2013;12(5):458.

53. Rasi Ghaemi S, Delalat B, Gronthos S, et al. High-Throughput Assessment and Modeling of a Polymer Library Regulating Human Dental Pulp-Derived Stem Cell Behavior. *ACS Applied Materials & Interfaces.* 2018;10(45):38739–38748.

54. Stanton AE, Tong X, Yang F. Extracellular matrix type modulates mechanotransduction of stem cells. *Acta Biomaterialia.* 2019;96:310–320.

55. Yu T-T, Cui F-Z, Meng Q-Y, et al. Influence of Surface Chemistry on Adhesion and Osteo/Odontogenic Differentiation of Dental Pulp Stem Cells. *ACS Biomaterials Science & Engineering.* 2017;3 (6):1119–1128.

56. Crowder Spencer W, Leonardo V, Whittaker T, Papathanasiou P, Stevens Molly M. Material cues as potent regulators of epigenetics and stem cell function. *Cell Stem Cell.* 2016;18(1):39–52.

57. Huebsch N. Translational mechanobiology: Designing synthetic hydrogel matrices for improved in vitro models and cell-based therapies. *Acta Biomaterialia.* 2019;94:97–111..

58. Murphy WL, McDevitt TC, Engler AJ. Materials as stem cell regulators. *Nature Materials.* 2014;13(6):547–557.

59. Hadden WJ, Young JL, Holle AW, et al. Stem cell migration and mechanotransduction on linear stiffness gradient hydrogels. *Proc Nat Acad Sci.* 2017;114(22):5647–5652..

60. Wong L, Kumar A, Gabela-Zuniga B, et al. Substrate stiffness directs diverging vascular fates. *Acta Biomaterialia.* 2019;96:321–329..

61. Yosef A, Kossover O, Mironi-Harpaz I, et al. Fibrinogen-Based Hydrogel Modulus and Ligand Density Effects on Cell Morphogenesis in Two-Dimensional and Three-Dimensional Cell Cultures. *Advanced Healthcare Materials.* 2019;8 (13):1801436.

62. Mazón P, García-Bernal D, Meseguer-Olmo L, Cragnolini F, De Aza PN. Human mesenchymal stem cell viability, proliferation and differentiation potential in response to ceramic chemistry and surface roughness. *Ceramics Int.* 2015;41(5, Part A):6631–6644.

63. Shen X, Ma P, Hu Y, Xu G, Zhou J, Cai K. Mesenchymal stem cell growth behavior on micro/nano hierarchical surfaces of titanium substrates. *Colloids Surf B Biointerfaces.* 2015;127:221–232.

64. Ekambaram BK, Niepel MS, Fuhrmann B, Schmidt G, Groth T. Introduction of laser interference lithography to make nanopatterned surfaces for fundamental studies on stem cell response. *ACS Biomat Sci Eng.* 2018;4(5):1820–1832.

65. Argentati C, Morena F, Montanucci P, et al. Surface hydrophilicity of poly(l-Lactide) acid polymer film changes the human adult adipose stem cell architecture. *Polymers.* 2018;10:2.

66. Jahani H, Jalilian FA, Wu C-Y, et al. Controlled surface morphology and hydrophilicity of polycaprolactone toward selective differentiation of mesenchymal stem cells to neural like cells. *J Biomed Mater Res A.* 2015;103(5):1875–1881.

67. Hao L, Fu X, Li T, et al. Surface chemistry from wettability and charge for the control of mesenchymal stem cell fate through self-assembled monolayers. *Colloids Surf B Biointerfaces.* 2016;148:549–556.

68. Tewary M, Shakiba N, Zandstra PW. Stem cell bioengineering: building from stem cell biology. *Nature Reviews Genetics.* 2018;19 (10):595–614.

69. Chu G, Yuan Z, Zhu C, et al. Substrate stiffness- and topography-dependent differentiation of annulus fibrosus-derived stem cells is regulated by Yes-associated protein. *Acta Biomaterialia.* 2019;92:254–264.

70. Haugh MG, Vaughan TJ, Madl CM, et al. Investigating the interplay between substrate stiffness and ligand chemistry in directing mesenchymal stem cell differentiation within 3D macro-porous substrates. *Biomaterials.* 2018;171:23–33..

71. Balikov DA, Fang B, Chun YW, et al. Directing lineage specification of human mesenchymal stem cells by decoupling electrical stimulation and physical patterning on unmodified graphene. *Nanoscale.* 2016;8(28):13730-13739.

72. Ribeiro AJS, Ang Y-S, Fu J-D, et al. Contractility of single cardiomyocytes differentiated from pluripotent stem cells depends on physiological shape and substrate stiffness. *Proceedings of the National Academy of Sciences.* 2015;112(41):12705.

73. Yang X, Xu Q. Bimetallic metal–organic frameworks for gas storage and separation. *Cryst Growth Des.* 2017;17(4):1450–1455.

74. Li H, Wang K, Sun Y, Lollar CT, Li J, Zhou H-C. Recent advances in gas storage and separation using metal–organic frameworks. *Materials Today.* 2018;21(2):108–121.

75. Sumida K, Rogow DL, Mason JA, et al. Carbon dioxide capture in metal–organic frameworks. *Chem Rev.* 2012;112(2):724–781.

76. Suh MP, Park HJ, Prasad TK, Lim D-W. Hydrogen storage in metal–organic frameworks. *Chem Rev.* 2012;112(2):782–835.

77. Hou J, Sutrisna PD, Wang T, et al. Unraveling the Interfacial Structure–Performance Correlation of Flexible Metal–Organic Framework Membranes on Polymeric Substrates. *ACS Applied Materials & Interfaces.* 2019;11(5):5570–5577.

78. Razmjou A, Asadnia M, Hosseini E, Habibnejad Korayem A, Chen V. Design principles of ion selective nanostructured membranes for the extraction of lithium ions. *Nat Commun.* 2019;10 (1):5793.

79. Hu Z, Deibert BJ, Li J. Luminescent metal–organic frameworks for chemical sensing and explosive detection. *Chem Soc Rev.* 2014;43 (16):5815–5840.

80. Kreno LE, Leong K, Farha OK, Allendorf M, Van Duyne RP, Hupp JT. Metal–organic framework materials as chemical sensors. *Chem Rev.* 2012;112(2):1105–1125.

81. Zhang Y, Yuan S, Day G, Wang X, Yang X, Zhou H-C. Luminescent sensors based on metal-organic frameworks. *Coord Chem Rev.* 2018;354:28–45.

82. Razmjou A, Asadnia M, Ghaebi O, et al. Preparation of iridescent 2D photonic crystals by using a mussel-inspired spatial patterning of ZIF-8 with potential applications in optical switch and chemical sensor. *ACS Appl Mater Interfaces.* 2017;9(43):38076–38080.

83. Liu J, Chen L, Cui H, Zhang J, Zhang L, Su C-Y. Applications of metal–organic frameworks in heterogeneous supramolecular catalysis. *Chem Soc Rev.* 2014;43(16):6011–6061.

84. Yoon M, Srirambalaji R, Kim K. Homochiral metal–organic frameworks for asymmetric heterogeneous catalysis. *Chem Rev.* 2012;112(2):1196–1231.

85. Huang Y-B, Liang J, Wang X-S CR. Multifunctional metal-organic framework catalysts: synergistic catalysis and tandem reactions. *Chem Soc Rev.* 2017;46(1):126–157.

86. Horcajada P, Gref R, Baati T, et al. Metal–organic frameworks in biomedicine. *Chem Rev.* 2011;112(2):1232–1268.

87. Simon-Yarza T, Mielcarek A, Couvreur P, Serre C. Nanoparticles of metal-organic frameworks: on the road to in vivo efficacy in biomedicine. *Adv Mater.* 2018;30(37):1707365.

88. Zheng Z, Chen Y, Guo B, et al. Magnesium-organic framework-based stimuli-responsive systems that optimize the bone microenvironment for enhanced bone regeneration. *Chem Eng J.* 2020;396:125241.

89. Shen X, Zhang Y, Ma P, et al. Fabrication of magnesium/zinc-metal organic framework on titanium implants to inhibit bacterial infection and promote bone regeneration. *Biomaterials.* 2019;212:1–16.

90. Dang W, Ma B, Li B, et al. 3D printing of metal-organic framework nanosheets-structured scaffolds with tumor therapy and bone construction. *Biofabrication.* 2020;12(2):025005.

91. Min H, Wang J, Qi Y, et al. Biomimetic metal–organic framework nanoparticles for cooperative combination of antiangiogenesis and photodynamic therapy for enhanced efficacy. *Adv Mater.* 2019;31(15):1808200.

92. Wang S, Chen Y, Wang S, Li P, Mirkin CA. DNA-functionalized metal–organic framework nanoparticles for intracellular delivery of proteins. *J Am Chem Soc.* 2019;141(6):2215–2219.

93. Qin L, Lin L-X, Fang Z-P, et al. A water-stable metal–organic framework of a zwitterionic carboxylate with dysprosium: a sensing platform for Ebolavirus RNA sequences. *Chem Commun.* 2016;52(1):132–135.

94. Hu Y, Cheng H, Zhao X, et al. Surface-enhanced Raman scattering active gold nanoparticles with enzyme-mimicking activities for measuring glucose and lactate in living tissues. *ACS Nano.* 2017;11(6):5558–5566.

95. Yang C, Chen K, Chen M, et al. Nanoscale metal–organic framework based two-photon sensing platform for bioimaging in live tissue. *Anal Chem.* 2019;91(4):2727–2733.

96. Zhang S, Pei X, Gao H, Chen S, Wang J. Metal-organic framework-based nanomaterials for biomedical applications. *Chine Chem Lett.* 2020;31(5):1060–1070.

97. Lu W, Wei Z, Gu Z-Y, et al. Tuning the structure and function of metal–organic frameworks via linker design. *Chem Soc Rev.* 2014;43(16):5561–5593.

98. Gkaniatsou E, Sicard C, Ricoux R, Mahy J-P, Steunou N, Serre C. Metal–organic frameworks: a novel host platform for enzymatic catalysis and detection. *Mater Horizons.* 2017;4(1):55–63.

99. Raja DS, Liu W-L, Huang H-Y, Lin C-H. Immobilization of protein on nanoporous metal-organic framework materials. *Comment Inorganic Chem.* 2015;35(6):331–349.

100. Yin Z, Wan S, Yang J, Kurmoo M, Zeng M-H. Recent advances in post-synthetic modification of metal–organic frameworks: new types and tandem reactions. *Coord Chem Rev.* 2019;378:500–512. doi:10.1016/j.ccr.2017.11.015

101. Mohammad M, Razmjou A, Liang K, Asadnia M, Chen V. Metal–Organic-Framework-Based Enzymatic Microfluidic Biosensor via Surface Patterning and Biomineralization. *ACS Applied Materials & Interfaces.* 2019;11(2):1807–1820.

102. Zare A, Bordbar A-K, Razmjou A, Jafarian F. The immobilization of Candida rugosa lipase on the modified polyethersulfone with MOF nanoparticles as an excellent performance bioreactor membrane. *Journal of Biotechnology.* 2019;289:55–63.

103. Kempahanumakkagari S, Kumar V, Samaddar P, Kumar P, Ramakrishnappa T, Kim K-H. Biomolecule-embedded metal-organic frameworks as an innovative sensing platform. *Biotechnology Advances.* 2018;36(2):467–481

104. Morris RE, Wheatley PS. Gas storage in nanoporous materials. *Angewandte Chem Int Edition.* 2008;47(27):4966–4981. doi:10.1002/anie.200703934

105. Keskin S, Kızılel S. Biomedical applications of metal organic frameworks. *Ind Eng Chem Res.* 2011;50(4):1799–1812. doi:10.1021/ie101312k

106. Jiang H-L, Makal TA, Zhou H-C. Interpenetration control in metal–organic frameworks for functional applications. *Coordination Chemistry Reviews.* 2013;257(15):2232–2249

107. Sun W, Zhai X, Zhao L. Synthesis of ZIF-8 and ZIF-67 nanocrystals with well-controllable size distribution through reverse microemulsions. *Chemical Engineering Journal.* 2016;289:59–64.

108. Shieh F-K, Wang S-C, Leo S-Y, Wu KCW. Water-Based Synthesis of Zeolitic Imidazolate Framework-90 (ZIF-90) with a Controllable Particle Size. *Chemistry – A European Journal.* 2013;19(34):11139–11142

109. Fairen-Jimenez D, Moggach SA, Wharmby MT, Wright PA, Parsons S, Düren T. Opening the Gate: Framework Flexibility in ZIF-8 Explored by Experiments and Simulations. *Journal of the American Chemical Society.* 2011;133(23):8900-8902.

110. Hou J, Sutrisna PD, Zhang Y, Chen V. Formation of ultrathin, continuous metal–organic framework membranes on flexible polymer substrates. *Angewandte Chemie International Edition.* 2016;55(12):3947–3951.

111. Liu Q, Wang N, Caro J, Huang A. Bio-Inspired Polydopamine: A Versatile and Powerful Platform for Covalent Synthesis of Molecular Sieve Membranes. *Journal of the American Chemical Society.* 2013;135(47):17679–17682

112. Wu Q, Niu M, Chen X, et al. Biocompatible and biodegradable zeolitic imidazolate framework/polydopamine nanocarriers for dual stimulus triggered tumor thermo-chemotherapy. *Biomaterials.* 2018/04/01/ 2018;162:132–143

113. Wong-Ng W, Kaduk JA, Espinal L, Suchomel MR, Allen AJ, Wu H. High-resolution synchrotron X-ray powder diffraction study of bis(2-methylimidazolyl)-zinc, C8H10N4Zn (ZIF-8). *Powder Diffraction.* 2012;26(3):234–237

114. Ebrahimi Dastgurdi M, Ejeian F, Nematollahi M, Motaghi A, Nasr-Esfahani MH. Comparison of two digestion strategies on characteristics and differentiation potential of human dental pulp stem cells. Archives of Oral Biology. 2018/09/01/ 2018

115. Liang W, Li L, Hou J, et al. Linking defects, hierarchical porosity generation and desalination performance in metal–organic frameworks. Chemical Science. 2018;9(14):3508–3516

116. Redfern LR, Farha OK. Mechanical properties of metal–organic frameworks. *Chemical Science.* 2019;10(46):10666-10679

117. Tan JC, Bennett TD, Cheetham AK, et al. Chemical structure, network topology, and porosity effects on the mechanical properties of Zeolitic Imidazolate Frameworks. *Proceedings of the National Academy of Sciences.* 2010;107(22):9938.

118. Li W, Henke S, Cheetham AK, et al. Research Update: Mechanical properties of metal-organic frameworks – Influence of structure and chemical bonding. *APL Materials.* 2014;2(12):123902.

119. Tan JC, Cheetham AKl. Mechanical properties of hybrid inorganic–organic framework materials: establishing fundamental structure–property relationships. *Chemical Society Reviews.* 2011;40(2):1059–1080.

120. Diring S, Carné-Sánchez A, Zhang J, et al. Light responsive metal–organic frameworks as controllable CO-releasing cell culture substrates. *Chem Sci.* 2017;8(3):2381–2386. doi:10.1039/C6SC04824B

121. Diring S, Wang DO, Kim C, et al. Localized cell stimulation by nitric oxide using a photoactive porous coordination polymer platform. *Nat Commun.* 2013;4(1):2684. doi:10.1038/ncomms3684

122. Telgerd MD, Sadeghinia M, Birhanu G, et al. Enhanced osteogenic differentiation of mesenchymal stem cells on metal–organic framework based on copper, zinc, and imidazole coated poly-l-lactic acid nanofiber scaffolds. *J Biomed Mater Res A*. 2019;107(8):1841–1848.

123. Liu Z, Tang M, Zhao J, Chai R, Kang J. Looking into the future: toward advanced 3D biomaterials for stem-cell-based regenerative medicine. *Adv Mater*. 2018;30(17):1705388. doi:10.1002/adma.201705388

124. Cavalcanti-Adam EA, Aydin D, Hirschfeld-Warneken VC, Spatz JP. Cell adhesion and response to synthetic nanopatterned environments by steering receptor clustering and spatial location. *HFSP J*. 2008;2(5):276–285. doi:10.2976/1.2976662

125. Marinkovic M, Dean DD, Chen X-D. Chapter 3 – maintenance and culture of MSCs. In: Chen X-D, editor. *A Roadmap to Non-Hematopoietic Stem Cell-Based Therapeutics: Academic Press*. 2019:39–61.

126. Bhattacharjee S, Jang M-S, Kwon H-J, Ahn W-S. Zeolitic imidazolate frameworks: synthesis, functionalization, and catalytic/adsorption applications. *Catalysis Surveys Asia*. 2014;18(4):101–127.

127. Ochsner M, Textor M, Vogel V, Smith ML. Dimensionality controls cytoskeleton assembly and metabolism of fibroblast cells in response to rigidity and shape. *PloS one*. 2010;5(3):e9445.

128. Yalak G, Shiu J-Y, Schoen I, Mitsi M, Vogel V. Phosphorylated fibronectin enhances cell attachment and upregulates mechanical cell functions. *PloS one*. 2019;14(7):e0218893.

129. Qazi TH, Hafeez S, Schmidt J, Duda GN, Boccaccini AR, Lippens E. Comparison of the effects of 45S5 and 1393 bioactive glass microparticles on hMSC behavior. *Journal of Biomedical Materials Research Part A*. 2017;105(10):2772-2782.

130. Gentleman MM, Gentleman E. The role of surface free energy in osteoblast–biomaterial interactions. *Int Mater Rev*. 2014;59(8):417–429. doi:10.1179/1743280414Y.0000000038

131. Caplan AI. Chapter 15 – mesenchymal stem cells in regenerative medicine. In: Atala A, Lanza R, Mikos AG, Nerem R, editors. *Principles of Regenerative Medicine (Third Edition)*. Boston: Academic Press; 2019:219–227.

132. Kobolak J, Dinnyes A, Memic A, Khademhosseini A, Mobasheri A. Mesenchymal stem cells: identification, phenotypic characterization, biological properties and potential for regenerative medicine through biomaterial micro-engineering of their niche. *Methods*. 2016;99:62–68. doi:10.1016/j.ymeth.2015.09.016

133. Ryan A, Murphy M, Barry F. *Mesenchymal Stem/Stromal Cell Therapy. The Biology and Therapeutic Application of Mesenchymal Cells*. Hoboken, New Jersey, USA: John Wiley & Sons, Inc; 2016:426–440.

134. Holm EM. *Bone Sialoprotein and Osteopontin Mediate Bone Development*. London, Ontario, Canada: Department of Biochemistry The University of Western Ontario; 2014.

135. Liu TM, Lee EH. Transcriptional regulatory cascades in Runx2-dependent bone development. *Tissue Eng Part B Rev*. 2013;19(3):254–263. doi:10.1089/ten.teb.2012.0527

136. Huebsch N, Arany PR, Mao AS, et al. Harnessing traction-mediated manipulation of the cell/matrix interface to control stem-cell fate. *Nat Mater*. 2010;9(6):518. doi:10.1038/nmat2732

137. Xu J, Sun M, Tan Y, et al. Effect of matrix stiffness on the proliferation and differentiation of umbilical cord mesenchymal stem cells. *Differentiation*. 2017;96:30-39.

138. Bunpetch V, Zhang Z-Y, Zhang X, et al. Strategies for MSC expansion and MSC-based microtissue for bone regeneration. *Biomaterials*. 2019;196:67-79.

139. Rao VV, Vu MK, Ma H, Killaars AR, Anseth KS. Rescuing mesenchymal stem cell regenerative properties on hydrogel substrates post serial expansion. *Bioengineering & Translational Medicine*. 2019;4(1):51-60.

140. Geiger B, Bershadsky A, Pankov R, Yamada KM. Transmembrane crosstalk between the extracellular matrix and the cytoskeleton. *Nature Reviews Molecular Cell Biology*. 2001;2(11):793-805.

141. Killaars AR, Grim JC, Walker CJ, Hushka EA, Brown TE, Anseth KS. Extended Exposure to Stiff Microenvironments Leads to Persistent Chromatin Remodeling in Human Mesenchymal Stem Cells. *Advanced Science*. 2019;6(3):1801483.

142. Gao L, McBeath R, Chen CS. Stem cell shape regulates a chondrogenic versus myogenic fate through Rac1 and N-Cadherin. *Stem Cells*. 2010;28(3):564–572.

143. Woods A, Beier F. RhoA/ROCK signaling regulates chondrogenesis in a context-dependent manner. *J Biol Chem*. 2006;281(19):13134–13140.

144. Langelier E, Suetterlin R, Hoemann CD, Aebi U, Buschmann MD. The chondrocyte cytoskeleton in mature articular cartilage: structure and distribution of actin, tubulin, and vimentin filaments. *J Histochem Cytochem*. 2000;48(10):1307–1320.

145. De Lucca L, da Costa Marques M, Weinfeld I, et al. Guided bone regeneration with polypropylene barrier in rabbit's calvaria: A preliminary experimental study. *Heliyon*. 2018;4(6):e00651.

146. Schendzielorz P, Rak K, Radeloff K, et al. A polydopamine peptide coating enables adipose-derived stem cell growth on the silicone surface of cochlear implant electrode arrays. *J Biomed Mater Res Part B:*. 2018;106(4):1431–1438.